The 2009 IEEE/RSJ International Conference on
Intelligent Robots and Systems
October 11-15, 2009 St. Louis, USA

A Compensated Sliding-window DFT Algorithm for Fine-grained Underwater Acoustic Ranging

Stephan Shatara and Xiaobo Tan

Abstract— **Fine-grained (sub-meter) ranging and localization is critical to the deployment of dense, mobile sensor networks in aquatic environments. However, such a task is faced with a number of challenges, including noisy underwater environments, limitation on size and complexity of localization hardware, and constraints on computing capabilities of sensor platforms. In this paper we present a sliding-window discrete Fourier transform (DFT)-based algorithm for precise detection of the arrival of a monotone acoustic signal, as a key enabling step in measuring the time of flight (TOF) of the acoustic signal for localization of the sensor node. The algorithm accommodates the rise dynamics of the signal and compensates for the latency in detection given the signal model, detection threshold, and steady-state signal amplitude. The algorithm is implemented onboard a small biomimetic robotic fish, and experiments in an indoor pool have shown that the proposed method results in an underwater ranging error of 1.4 wavelengths (74.3 cm), and is thus promising for localization of dense aquatic networks. The proposed method has also shown robustness in comparison with other tested methods including a matched filter-type method.**

I. INTRODUCTION

With the advances in underwater robotics and wireless networking, there is a growing interest in developing and deploying dense (1 - 100 m separation), mobile, aquatic sensor networks [1]. Such sensor networks can be used to collect temporally and spatially resolved information in aquatic environments, with applications in oceanography, marine biology, pollution detection, seismic monitoring, oil/gas field exploration, and aquafarm monitoring. Of particular interest are robotic fish-based platforms that are small (decimeter scale), inexpensive, and energy-efficient, and are thus affordable and easy to deploy in large numbers.

For small robotic fish, having onboard localization capability is essential for successful navigation of the robot and for effective coordination of robotic fish network. Accurate localization is also critical for tagging the sensed information so that the data collected by robotic fish are associated correctly to the physical location in the water. It is often desirable to achieve *GPS-free* localization, because the precision of commercially available GPS units (5 - 10 m) is inadequate for many applications, where sub-meter localization precision is needed. Furthermore, GPS signals are often unavailable due to their rapid attenuation underwater.

A number of GPS-free localization approaches has been proposed, involving the use of optical (infrared or visible), acoustic, or RF signals. Node localization within the network is typically achieved through two phases: 1) range estimation (i.e., ranging) or bearing angle estimation, and 2) translation of range and/or angle estimates into a position through geometric relations [2]. Ranging can be realized using the received signal strength information (RSSI) [3]. RADAR [4] and SpotOn [5] are two examples of RF RSSI-based ranging. But it is well documented that this approach is not reliable in cluttered or noisy environments. Another major approach in ranging is to measure the time of signal propagation, such as Time of Flight (TOF). The TOF measurement is often made with acoustic (including ultrasonic) signals, synchronized through RF communication. Examples of TOF-based methods include AHLoS [6], the Cricket location-support system [7], and the Calamari system [8]. Measurement of Angle of Arrival (AOA) is another common approach in localization [9], [10]; however, extracting angles of arrival requires receiver arrays, increasing hardware requirements thus making AOA unfavorable in small robotic fish where space and resources are limited.

The aforementioned methods are mostly studied for localization in air. Onboard localization for small robotic fish presents many new challenges. First, comparing to in-air localization, underwater localization itself is much more difficult. RF signals have large attenuation in water. The influence of currents, depth, temperature and salinity on sound speed [11] inevitably introduces error in the estimation of travel distance of the acoustic signal. Second, the relatively low speed (typically under 50 cm/s) and the size of the small robotic fish demand high resolution (1 m or less) in localization. Finally, the constraints on power, size, and weight require that the onboard localization system has minimal volume and computational complexity. While underwater localization and its related topics (in particular, the sonar technology) have been studied for almost a century [12], [13], the requirements there on ranging/localization resolution and the constraints on power/sizes of acoustic transceivers are in general much more relaxed. For example, the system reported in [14] used powerful hydrophones as tranceivers and full-fledged computer systems for signal analysis, both of which would be unavailable for small robotic fish.

In this paper we present a TOF-based underwater acoustic ranging scheme targeting small robotic fish with inexpensive

This work was supported in part by ONR (grant N000140810640, program manager Dr. T. McKenna) and NSF (ECCS 0547131, CCF 0820220).

S. Shatara is with Motorola, 1301 E. Algonquin Rd, Schaumburg, IL 60196, USA. X. Tan is with the Smart Microsystems Laboratory, Department of Electrical and Computer Engineering, Michigan State University, East Lansing, MI 48824, USA. s.shatara@motorola.com (S. S.), xbtan@egr.msu.edu (X. T.)

Send correspondence to X. Tan. Tel: 517-432-5671; Fax: 517-353-1980.

hardware. Although ultrasonic signals are a popular choice for TOF-based ranging [6], [7], their high directionality requires multiple transceivers to remove blind spots, making them unfavorable for size-constrained robotic fish. Instead, we have adopted a monotone, audible signal (2.8 kHz), produced by a sounder (buzzer) and received by a microphone. The major challenge in estimating the TOF is precise determination of the arrival instant of ranging signal, in the presence of signal transients, signal attenuation, and ambient noises, using limited onboard hardware and computational capability. An efficient, robust, sliding-window discrete Fourier transform (SDFT) algorithm is proposed to address this challenge. The algorithm computes and monitors the signal component of desired frequency in real time, and reports detection once the component exceeds a prespecified threshold. To further accommodate the effect of signal transients, the rise dynamics of signal is modeled and its influence on detection latency derived, which is then compensated in the proposed algorithm.

The proposed algorithm is implemented onboard a biomimetic robotic fish. Experiments in an indoor pool have shown that the underwater ranging error of the proposed SDFT-based method is within 1.4 wavelengths (74.3 cm) of the acoustic signal. In terms of the number of wavelengths, the performance has even surpassed the state of the art in in-air ranging methods (2.3 wavelengths) [7], [15]. Experimental results have also shown that the SDFT-based method is robust in comparison with three other tested methods for detection of signal arrival, which are based respectively on a) threshold-crossing of instantaneous signal magnitude, b) a tone detection circuit, and c) matched filter-type correlation.

The remainder of this paper is organized as follows. Section II is a brief overview of the robotic fish-based mobile platform, ranging hardware, and TOF-based ranging protocol implemented on-board the robotic fish. The SDFT algorithm is presented in Section III, along with the discussion on the compensation function. Experimental ranging results using the proposed SDFT scheme and three other methods are discussed in Section IV. Conclusions are provided in Section V.

II. Description of the Ranging System

A. Platform Hardware

Ranging is performed onboard a mobile platform in the form of a robotic fish, representing a node for eventual deployment as part of a dynamic sensor network. Shown in Fig. 1 is a robotic fish prototype, upgraded from that reported in [16]. The robotic fish is propelled by an ionic polymer-metal composite (IPMC) actuator as a caudal fin. The addition of a passive fin to the IPMC piece is used to enhance propulsion, and consequently the steady-state velocity [17]. The electronics and lithium-ion batteries are housed in a waterproof casing placed within a custom-made fiberglass outer shell.

The prototype is controlled by a 16-bit digital signal controller (DSC) (dsPIC30F3012, Microchip), where all the control and computational processes originate. Amongst the peripherals attached to the DSC is a ZigBee-standard RF transceiver (XBee, Digi/Maxstream), used for wireless communications and generating the RF packet in the ranging protocol. The robotic fish is also fitted with a piezoelectric buzzer (CPE-267, CUI Inc.) and an electret condenser microphone (WP23502, Knowles Acoustics), used in the generation and detection respectively of the acoustic pulse. Both components are chosen based on their performance specifications, size, weight, and price. Routed through a 12 V DC-DC step up converter (MAX761, Maxim), a signal from the DSC controls the pulse duration of the buzzer, producing a monotone signal with a center frequency f_0 of 2.8 kHz. On the receiving end, the signal from the microphone is amplified and filtered using active bandpass circuitry, before being sampled by the DSC at a rate of $F_s = 88.76$ kHz.

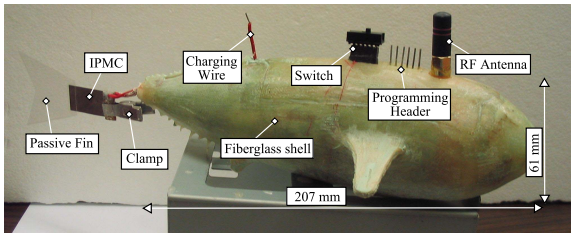

Fig. 1. An aquatic sensor platform based on a biomimetic robotic fish propelled by an IPMC caudal fin.

B. TOF-Based Ranging Protocol

In this paper ranging is achieved through the measurement of time of flight (TOF), by concurrent use of an RF packet and an acoustic pulse. It is assumed that the RF packet is received instantaneously; error induced by such an assumption is about 0.5 mm for a node separation distance of 100 m. Since RF signals propagate poorly underwater, the ranging and thus localization is only performed when the robotic fish surfaces with its RF antenna exposed in air (but buzzer and microphone still underwater). Note that, however, the proposed method for detection of sound arrival is applicable in general cases and not limited to the case of RF-enabled synchronization and thus not limited to ranging/localization on water surface. Ranging between two nodes is performed using the following protocol:

- Step 1: Node 1 transmits an RF packet to Node 2 to indicate it is ready;
- Step 2: Node 2 simultaneously transmits an RF packet and an acoustic pulse;
- Step 3: Node 1 receives the RF packet and starts on-board timer;
- Step 4: Node 1 receives the acoustic pulse and stops on-board timer;
- Step 5: Distance between receiver and transmitter is estimated from the timer reading.

Although seemingly straightforward, accurately determining the arrival of the acoustic signal (Step 4) is challenging due to signal transients, various noises, multi-path effects, and hardware constraints. While not a central issue in air,

precise detection of the arrival moment is critical underwater as every missed signal cycle introduces errors of approximately 53.6 cm. This is the central problem the paper aims to address.

III. Sliding-window DFT (SDFT) Algorithm

A. Derivation of SDFT

The short-term Fourier transform (STFT) [18] is based on the discrete Fourier transform (DFT), with the addition of time dependency,

$$X_{STFT}[k,n] = \sum_{m=0}^{R-1} x[n-m]w[m]e^{-j\frac{2\pi k}{N}m}, \quad 0 \le k \le N-1, \quad (1)$$

where n represents the discrete time, index k identifies the frequency bins $f = \frac{kF_s}{N}$, N is the Fourier sequence length, and F_s is the sampling frequency for obtaining $x[\cdot]$. R is the size of the window sequence $w[\cdot]$ that extracts a finite portion of $x[\cdot]$ for analysis; such an operation makes the signal approximately stationary over the specified section.

With the buzzer producing a monotonic signal with known center frequency f_0, we can focus on a single frequency bin $k = p = \left[\frac{f_0 N}{F_s}\right]$, where the result in $[\cdot]$ is rounded to the nearest integer. We can further simplify the STFT by using a rectangular window sequence ($w[\cdot] = 1$) with length $R = N$,

$$X_p[n] = \sum_{m=0}^{N-1} gx[n-m]e^{-j\omega_0 m}, \quad (2)$$

where $\omega_0 \triangleq \frac{2\pi p}{N}$ and $0 < g \le 1$ is some software-selectable gain. The parameter g is introduced for convenience in tuning the computation in onboard implementation, and it has no significance in the analysis here. Associated with the STFT algorithm is the overlapping of the samples $x[\cdot]$ within the consecutive windows, which results in a recursive algorithm, termed as SDFT, as follows:

$$X_p[n] = e^{-j\omega_0}X_p[n-1] + gx[n] - ge^{-j\omega_0}x[n-N]. \quad (3)$$

The resulting sequence $X_p[\cdot]$ is complex, for which the algorithm needs to compute the magnitude for monitoring purposes. Due to the complexity of implementing square root functions using the DSC, the algorithm instead monitors $\left|X_p[\cdot]\right|^2$, which defines the power density at f_0, with an additional factor of 2π. From here on, the term *power density* is used interchangeably with $\left|X_p[\cdot]\right|^2$. Upon arrival of the signal, the power density increases and crosses a software-selectable threshold ε,

$$\left|X_p[n]\right|^2 \ge \varepsilon, \quad (4)$$

at which point the algorithm is immediately stopped and the time n recorded. The recorded value corresponds to the propagation time between the transmitter-receiver pair.

B. Ideal Case: Steady-State Signal

Next we analyze properties of the SDFT algorithm relevant to the error in the detection of signal arrival. Analysis is provided for two cases, the first being the ideal case where the signal arrives with steady-state amplitude. The second is the non-ideal case, where the arriving signal has some transient dynamics. Note that $X_p[n]$ depends on the samples in a window ending with $x[n]$. Ignoring the ambient noise, we note that the samples in a window of size N will be zero until the signal arrives. Let s be the number of samples in the window that belong to the acoustic signal, with $0 \le s \le N$. Relabeling the samples in a window by q, $q = 0, \cdots, N-1$, we can express them as

$$x'[q] = \begin{cases} 0, & \text{if } q < N-s, \\ AE[q-(N-s)]\sin(\omega_0(q-(N-s))), & \text{otherwise.} \end{cases} \quad (5)$$

In (5), A is the steady-state amplitude of the acoustic signal, and $E[\cdot]$ represents an envelope function. For the ideal case, $E[\cdot] \equiv 1$. Fig. 2 illustrates the definition of $x'[q]$. Note the relationship between $x'[\cdot]$ and the original sequence $x[\cdot]$:

$$x'[q] = x[n+q-(N-1)]. \quad (6)$$

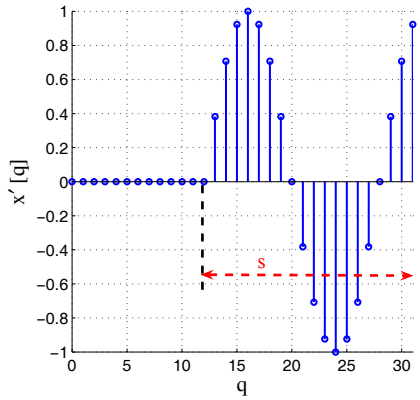

Fig. 2. Illustration of the windowed samples from an arriving signal with steady-state amplitude. Here $A = 1$, $N = 32$, and $s = 20$.

Using (2), (5), and (6), we can derive $|X_p[n]|^2$ as a function of s:

$$|X_p[n]|^2 = \frac{A^2}{4}\left[\left(\sum_{l=0}^{s-1}\sin(\alpha l)\right)^2 + \left(s - \sum_{l=0}^{s-1}\cos(\alpha l)\right)^2\right], \quad (7)$$

where $\alpha = 2\omega_0$. From (7), the power density is an accumulation of the sampled arriving signal, suggesting that some latency is necessary before reaching a given threshold. The dependence of such a latency on the amplitude A is also evident from (7).

Fig. 3 illustrates the above analysis. For an ideal sinusoidal signal arriving at $t_0 = 0$, $|X_p[l]|^2$ rises gradually after $t_0 = 0$, following (7). The power density saturates when the window includes p cycles. The latency in detection due to the threshold ε is also highlighted, requiring some non-zero time $t_1 > t_0$. For example, for $\varepsilon = 2000$, $t_1 = 83$ samples, or 62.25

cm of error for $F_s = 200$ kHz. The analysis demonstrates that even in the ideal case, joint time-frequency analysis of an arriving signal introduces timing error that needs to be compensated.

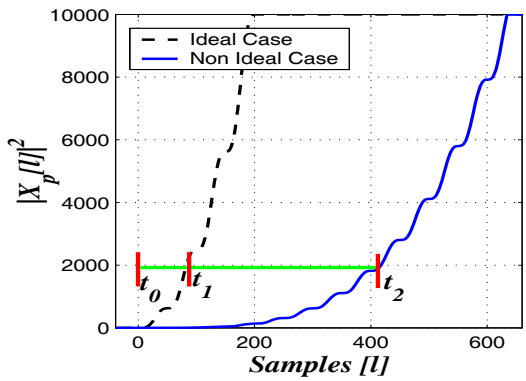

Fig. 3. Evolution of the computed power density for ideal and non-ideal signals. Here $N = 200, p = 2, A = 1$. Note the latency in detection for both cases.

C. Non-Ideal Case: Presence of Signal Transient

Next we investigate the effect of signal rise dynamics on the recursively evaluated power density. A sample of the microphone signal is shown in Fig. 4. It can be seen that, due to transducer characteristics, there is a transient before the amplitude of signal reaches the steady state. The rise dynamics can be approximately treated as a first-order system. Accordingly, the envelope function $E(\cdot)$ in (5) can be expressed as

$$E[l] = 1 - e^{\beta l}, \tag{8}$$

where $\beta \triangleq -\frac{T_s}{\tau}$ and $T_s = \frac{1}{F_s}$ is the sampling interval. The rise constant τ can be identified empirically through data fitting. Fig. 4 shows that the rising amplitude can be approximated with a first-order system with $\tau = 0.004$ s.

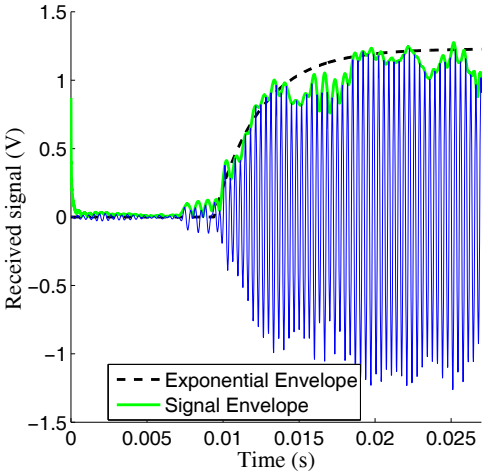

Fig. 4. Sampled acoustic signal underwater showing transient characteristics.

Similar as in the ideal case, we can derive $|X_p^n|^2$ for the non-ideal case, in terms of s:

$$|X_p[n]|^2 = \frac{A^2}{4}\left[\left(\sum_{l=0}^{s-1}(1-e^{\beta l})\sin(\alpha l)\right)^2 + \left(\sum_{l=0}^{s-1}(1-e^{\beta l})(1-\cos(\alpha l))\right)^2\right]. \tag{9}$$

The simulation result based on (9) is shown in Fig. 3, and as expected, we see that detection latency $t_2 > t_0$ due to signal transients is even greater than that in the ideal case. The value of τ affects the delay t_2 in that the accumulation rate becomes lower as the rise constant increases. For $A = 1$, $\varepsilon = 2000$, the latency is $t_2 = 416$ samples, which is equivalent to a ranging error of 312 cm for $F_s = 200$ kHz if uncompensated. The potentially significant error necessitates a compensation step to remove the latency.

D. Onboard Compensation of Latency

For a given ε, Eq. (7) and (9) show that it will take some $s = s^* > 0$ for $|X_p^s|^2$ to cross the threshold ε, for both the ideal and non-ideal cases. For either case, the number of samples s^* would represent the latency in the detection of signal arrival. The idea of compensation is to subtract s^* off the timer reading, thus removing the latency introduced by the algorithmic artifact.

We will focus on the non-ideal case, since that is what one encounters in reality. The value s^* of latency is a function of ε, τ, and A, as determined by (9). However, given $|X_p^s|^2 = \varepsilon$, the nonlinear equation (9) is difficult to solve for s. Instead, for a given ε and the experimentally identified rise constant τ, and for a range of values A, we evaluate (9) in Matlab and locate s^* at threshold crossing for each value of A. A look-up table is then created and stored onboard the robotic fish, which can efficiently provide the compensation value once the signal amplitude A is known, eliminating the need of intensive computation onboard.

The following method has been adopted to measure the steady-state signal amplitude A online. Prior to ranging, the buzzer transmits a 100 ms pulse, which the receiving node records after a specified amount of time (to ensure steady-state amplitude is reached). To compute A, the receiving node takes the sum of absolute values of the incoming signal samples,

$$\widetilde{A} = \frac{g}{N}\sum_{n=0}^{N-1}|x[l]|. \tag{10}$$

Since $x[\cdot]$ is a sinusoidal signal with amplitude A,

$$\widetilde{A} = \frac{2Agp}{N}\left(1 + \frac{\sin(\alpha/2)}{1-\cos(\alpha/2)}\right), \tag{11}$$

which allows evaluation of A using the measurement $\widetilde{A}$.

IV. Experimental Results on Ranging

A. Results of the SDFT-based Ranging Scheme

Experiments were mostly conducted across the width of the deep side of an indoor pool. The pool has dimensions

13×25 m^2, with depth varying from 1.3 m to 3.3 m. For the SDFT scheme, the ranging sequence for a single measurement involves a 100 ms pulse for computing steady state amplitude A, followed by a 35 ms pulse for actual range estimation, with 500 ms wait period between the two. Consecutive ranging sequences have a wait period of 1500 ms to avoid reverberant noise in the recorded signal. At each distance increment of 91.44 cm, the amplitude, compensated range estimate, and compensation value are recorded ten times, and the mean is taken of each data set as the final estimate. The ranging results, including the measured signal amplitude at the steady state, are shown in Fig. 5.

Consistent with the analytical results for the non-ideal case, Fig. 5 shows that the uncompensated range estimates can have large errors (over 300 cm). We observe the relationship between the uncompensated estimate and the recorded signal amplitude; as the amplitude drops with range, the absolute error of the uncompensated range estimate increases, which is consistent with the analysis (9). After compensation, the absolute error reduces to less than 1.4 wavelengths (74.3 cm) over a range exceeding 10 m. Judging in the number of wavelengths, we note that the error under SDFT with compensation for underwater ranging is even smaller than the error in TOF-based in-air ranging using 40 kHz ultrasonic signals, which has 2.3 wavelengths. It is expected that, due to the construction of the SDFT algorithm, its ranging error would be independent of the signal frequency and thus the number of wavelengths is a reasonable metric.

B. Comparison with Other Methods

The SDFT-based method is also compared to three other methods for detecting the arrival of the acoustic signal: a) the threshold-crossing method compares the pre-processed microphone signal with a threshold and reports detection once the threshold is crossed, b) the tone-detection method uses a tone detector chip (LMC567, National Semiconductor) tuned to 2.8 kHz, which declares signal arrival once the internal phase locked loop (PLL) is locked, and c) the correlation method, which monitors the integral of the product of V_{mic} and a template sinusoidal signal $\sin(\omega t)$ with frequency 2.8 kHz. Details of these three methods can be found in [19].

As hardware-based approaches, the threshold-crossing method and the tone-detection methods were implemented on an earlier prototype of robotic fish [19], while the correlation method, which requires digital signal processing, was implemented in the prototype shown in Fig. 1. As shown in [19], with the threshold-crossing method, the measured ranges for each fixed distance were highly scattered, implying its great susceptibility to noise. The maximum ranging error was about 90 cm over the range of 500 cm (beyond which the signal was barely distinguishable from the noise). With the tone-detection method, the ranging error was mostly under 130 cm (maximum 180 cm) for a range of about 1000 cm [19]. The raw data for each fixed distance were also scattered. Part of the reason for the uncertainty in lock-on times is that the frequency of the buzzer is not strictly constant;

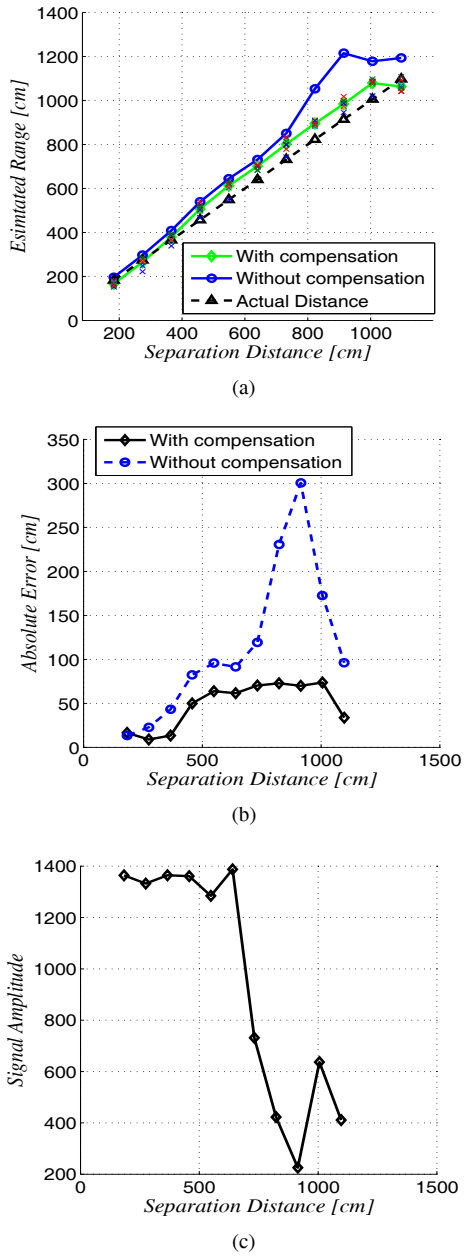

Fig. 5. Experimental results on ranging underwater using the SDFT method. (a) Estimated distance versus actual distance; (b) absolute error with and without compensation; (c) measured steady state amplitude A.

experimental data have shown a standard deviation of 90.4 Hz from the nominal frequency of 2.8 kHz.

For the correlation method, ranging results were collected at five different transmitter-receiver separation distances, as seen in Fig. 6. At each point, 10 range estimates were made using 20 ms pulses, and the mean of the estimates was taken as the final estimate. The absolute error in ranging is less than 120 cm over a range of about 1000 cm. Note that there is still a large variation in the measurement results. A major cause of the uncertainty is attributed to the unknown deviation slope of the correlation integral [20].

From the discussions above, we can see that the proposed

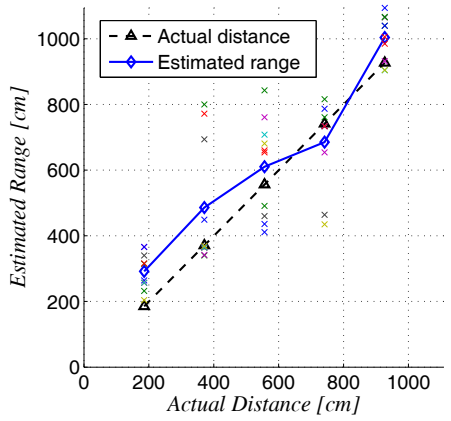

Fig. 6. Experimental results on ranging underwater using the correlation method.

SDFT-based method not only produces the least amount of ranging error, but also is far more consistent than other methods. In particular, as seen in Fig. 5(a), the range estimates for each fixed distance under the proposed method have little scattering, showing the robustness of the SDFT scheme against noise and other uncertainties.

V. Conclusion

In this paper we have presented an effective underwater ranging method for small robotic fish, as an important step towards GPS-free localization of these robots in aquatic sensing applications. A monotone buzzer and a single microphone were adopted for production and detection of the acoustic signal, to accommodate the requirements of low cost, compact size, and low computational complexity for the robot. While the use of a richer acoustic signal and/or multiple microphones could facilitate more accurate ranging, it was not studied considering the associated cost and complexity. A key component of the proposed ranging scheme was a compensated sliding-window DFT algorithm for precise detection of the arrival of acoustic signal, in the presence of ambient noises and signal transients, with limited computational resources. Through comparison with three other methods, we have established the advantages of the proposed scheme in both accuracy and robustness.

In future work experiments will be performed in a larger aquatic environment (e.g., a lake) to examine the maximum ranging distance under the current system, and to investigate ways for extending the distance. We will also carry out more extensive localization experiments, where groups of robotic fish use their onboard localization system to demonstrate collaborative behaviors. Another aspect of future work is to accommodate synchronization without the use of RF, for example, by exploring the use of acoustic communication. This would remove the current constraint that the localization is only performed when the robotic fish surfaces.

Acknowledgment

The authors would like to thank Bryan Thomas, Nathan Gingery, and Stephan Henneberger for their help in implementing the ranging methods reported in this paper, and John Thon for arranging pool access for the experiments.

References

[1] J. H. Cui, J. Kong, M. Gerla, and S. Zhou, "Challenges: Building scalable mobile underwater wireless sensor networks for aquatic applications," *IEEE Network*, vol. 20, no. 3, pp. 12–18, 2006.

[2] J. Gibson, *Mobile Communications Handbook*, 2nd ed. Boca Raton, FL: CRC, 1999.

[3] K. Whitehouse, C. Karlof, and D. Culler, "A practical evaluation of radio signal strength for ranging-based localization," *ACM SIGMOBILE Mobile Computing and Communication Review*, vol. 11, no. 1, pp. 41–52, 2007.

[4] P. Bahl and V. N. Padmanabhan, "RADAR: An in-building RF-based user location and tracking system," in *Proceedings of the Nineteenth Annual Joint Conference of the IEEE Computer and Communications Societies (INFOCOM 2000)*, 2000, pp. 775–784.

[5] J. Hightower, C. Vakili, G. Borriello, and R. Want, "Design and calibration of the SpotON ad-hoc location sensing system," University of Washington, Tech. Rep., 2001, available at citeseer.ist.psu.edu/479904.html.

[6] A. Savvides, C.-C. Han, and M. B. Strivastava, "Dynamic fine-grained localization in ad-hoc networks of sensors," in *Proceedings of the 7th Annual International Conference on Mobile Computing and Networking*, 2001, pp. 166–179.

[7] N. B. Priyantha, A. Chakraborty, and H. Balakrishnan, "The Cricket location-support system," in *Proceedings of the 6th Annual International Conference on Mobile Computing and Networking*, 2000, pp. 32–43.

[8] C. D. Whitehouse, "The design of Calamari: An ad-hoc localization system for sensor networks," Master's thesis, University of California, Berkeley, 2002.

[9] D. Niculescu and B. Nath, "Ad hoc positioning system (APS) using AOA," in *Proceedings of the Twenty-Second Annual Joint Conference of the IEEE Computer and Communications Societies (INFOCOM 2003)*, 2003, pp. 1734–1743.

[10] P. Rong and M. L. Sichitiu, "Angle of arrival localization for wireless sensor networks," in *Proceedings of the 3rd Annual IEEE Communications Society Conference on Sensor and Ad Hoc Communications and Networks*, 2006, pp. 374–382.

[11] H. Medwin, "Speed of sound in water for realistic parameters," *Journal of Acoustical Society of America*, vol. 58, p. 1318, 1975.

[12] A. B. Wood and H. E. Browne, "A radio-acoustic method of locating positions at sea: Application to navigation and to hydrographical survey," *Proceedings of the Physical Society of London*, vol. 35, no. 1, pp. 183–193, 1922.

[13] A. Quazi, "An overview on the time delay estimate in active and passive systems for target localization," *IEEE Transactions on Acoustics, Speech, and Signal Processing*, vol. 29, no. 3, pp. 527–533, 1981.

[14] N. Kottege and U. R. Zimmer, "Relative localisation for AUV swarms," in *Proceedings of the Symposium on Underwater Technology and Workshop on Scientific Use of Submarine Cables and Related Technologies*, 2007, pp. 588–593.

[15] A. Ward, A. Jones, and A. Hopper, "A new location technique for the active office," *IEEE Personal Communications*, vol. 4, no. 5, pp. 42–47, 1997.

[16] X. Tan, D. Kim, N. Usher, D. Laboy, J.Jackson, A.Kapetanovic, J. Rapai, B. Sabadus, and X. Zhou, "An autonomous robotic fish for mobile sensing," in *Proceedings of the IEEE/RSJ International Conference on Intelligent Robots and Systems*, Beijing, China, 2006, pp. 5424–5429.

[17] E. Mbemmo, Z. Chen, S. Shatara, and X. Tan, "Modeling of biomimetic robotic fish propelled by an ionic polymer-metal composite actuator," in *Proceedings of the 2008 IEEE International Conference on Robotics and Automation*, Pasadena, CA, 2008, pp. 712–717.

[18] S. Mitra, *Digital Signal Processing: A Computer-Based Approach*, 2nd ed. Boston: McGraw-Hill, 2001.

[19] S. Shatara, X. Tan, E. Mbemmo, N. Gingery, and S. Henneberger, "Experimental investigation on underwater acoustic ranging for small robotic fish," in *Proceedings of the 2008 IEEE International Conference on Robotics and Automation*, Pasadena, CA, 2008, pp. 712–717.

[20] S. Shatara, "Development of small biomimetic robotic fish with onboard fine-grained localization," Master's thesis, Michigan State University, East Lansing, MI, 2008.